Model for Reggeon-Pomeranchukon cuts

Swee-Ping Chia*
International Centre for Theoretical Physics, Trieste, Italy
(Received 16 September 1975)

A model is presented for calculating Reggeon-Pomeranchukon cuts, making use explicitly of the Mandelstam diagram. External spins are treated in a natural way. Calculation for the general case is outlined and it is shown that in practical application the cut can be calculated in a standard way. Cuts associated with the exchanges of π, ρ, B, and A_2 are considered, and characteristics of the RP cuts, as well as the structure functions, are extracted and discussed. It is found that the model differs considerably from the absorption model. Two suppression schemes are operative which control the magnitudes of cut contributions to amplitudes with "naturality" opposite to the Reggeon. The πP cut is found to be a unique case because of the smallness of the pion mass. In general, the RP cuts are self-conspiratorial. At very high energies, all cuts, except πP cut, exhibit quasifactorization.

I. INTRODUCTION

It has been known for quite some time that cuts in the complex j plane, Regge cuts, are necessary for the description of hadronic scattering processes. The most obvious example is the sharp forward spike observed in the processes $np \to pn$ and $\gamma p \to \pi^+ n$, which are dominated by π exchange near the forward direction. The π Reggeon, being evasive, cannot explain the forward spike. The conspirator model,[1-3] which explains the forward spike by assuming conspiracy between the π Reggeon and its conspirator π_c, is not compatible with factorization.[4,5] Regge cut is therefore the only natural explanation.

Unfortunately, there is as yet no agreed way of calculating Regge cuts. The absorption model,[6] which generates Reggeon-Pomeranchukon cuts through absorptive corrections, has some success but is unable to explain the fine details of the πN charge-exchange (CEX) reaction. The failure is generally attributed to the lack of structure of the Pomeranchukon used. Several remedies to the conventional absorption model have since been suggested, such as the Pomeranchukon model of Hartley and Kane[7] and the phase-modified cuts,[8] but they are unattractive.

In this paper we present an alternative method of calculating Reggeon-Pomeranchukon (RP) cuts. The cuts are generated explicitly from the Mandelstam diagram,[9] with spins explicitly treated in a natural way. The model (herein referred to as the *diagram model*) was first used to generate the πP cut and was successful in explaining many features of π-exchange reactions.[10,11] A preliminary fit to the πN charge-exchange data also shows reasonable agreement.[12]

The purpose of this paper is to present the model and to extract from it some common characteristics of the RP cuts. To do this, we have investigated cuts associated with four different exchanges, π, ρ, B, and A_2, together with a large class of reactions controlled by such exchanges. A reaction is identified by its two vertices, e.g. $\pi N \to \rho N$ is identified by the vertices $\pi\rho$ and NN. When the exchange is intended to be explicitly mentioned, we shall use the notations $(\pi)\pi\rho$ and $(\pi)NN$, where it is understood that the symbol inside the brackets denotes the exchange. To be general, we have considered the following representative list of vertices: NN, $N\Delta$, $\pi\pi$, $\pi\eta$, $\pi\rho$, πB, πf, and πA_2.

II. THE MODEL

In formulating the model we are guided by the general requirement that the input ansatz for the RP cut in a particular reaction must be the same Reggeon exchange to the same reaction. The simplest way to realize this requirement over a large class of reactions is to assume that, in the Mandelstam diagram, the exchange Pomeranchukon is linked to the external hadrons via isoscalar-scalar "σ" particles.[10] We therefore depict the following physical picture for the RP cut as shown in Fig. 1. The incoming hadrons, on passing by each other, each emit a σ particle. The σ particles then scatter via Pomeranchukon exchange, while the virtual hadrons interact via Reggeon exchange. The σ particles are subsequently absorbed by the outgoing hadrons.

Since the Pomeranchukon exchange enters via the scattering of spinless σ particles, it takes on the simple form

$$F^{(P)}(s,\tau) = -\gamma_P{}^2 \exp(-A_P\tau)(-is)^{\phi_P(\tau)}, \qquad (2.1)$$

with the trajectory function given by $\phi_P(\tau) = 1 - \phi_P'\tau$. Hereinafter, the variable $\tau = -t$ will be used instead of the conventional t. It will be seen that with a Pomeranchukon exchange as simple as (2.1) we are able to obtain structure in the resulting RP cut. The structure comes from the crosses.

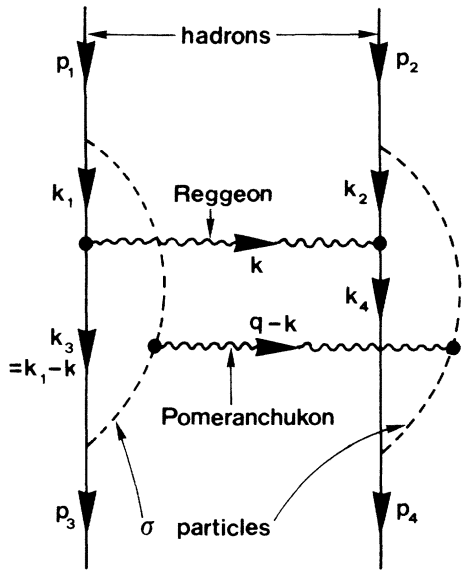

FIG. 1. Physical picture of the Mandelstam diagram, showing emission and reabsorption of the σ particles by the hadrons. Virtual hadrons interact via Reggeon exchange, while σ particles scatter via Pomeranchukon exchange.

The Reggeon exchange in the process $p_1+p_2\to p_3+p_4$ is assumed to be

$$F^{(R)}_{\{\lambda\}}(s,\tau)=B_{\{\lambda\}}(m_R{}^2+\tau)^{-1}\exp[-A_R(m_R{}^2+\tau)]\times(-is)^{\phi_R(\tau)-j_R}, \tag{2.2}$$

where $\phi_R(\tau)=j_R-\phi'_R(m_R{}^2+\tau)$ is the trajectory function and m_R and j_R are, respectively, the mass and spin of the lowest-lying recurrence on the trajectory. The propagator-like denominator, $(m_R{}^2+\tau)^{-1}$, comes from the long-range force of the Reggeon exchange. The helicity structure is contained in the *residue* functions $B_{\{\lambda\}}$ which are expressed as products of the *vertex functions*

$$B_{\{\lambda\}}=V^L_{\lambda_3\lambda_1}\cdot V^R_{\lambda_4\lambda_2}, \tag{2.3}$$

where the dot represents symbolically the product

$$\begin{aligned} V^L\cdot V^R &= V^LV^R \text{ for } j_R=0,\\ &=(V^L)^\mu P_{\mu\nu}(q)(V^R)^\nu \text{ for } j_R=1, \text{ and}\\ &=(V^L)^{\mu\nu}\Sigma_{\mu\nu\rho\sigma}(q)(V^R)^{\rho\sigma} \text{ for } j_R=2, \end{aligned} \tag{2.4}$$

where

$$P_{\mu\nu}(q)=-g_{\mu\nu}+q_\mu q_\nu/m_R{}^2, \tag{2.5}$$

$$\Sigma_{\mu\nu\rho\sigma}(q)=\tfrac{1}{2}P_{\mu\rho}(q)P_{\nu\sigma}(q)+\tfrac{1}{2}P_{\mu\sigma}(q)P_{\nu\rho}(q)-\tfrac{1}{3}P_{\mu\nu}(q)P_{\rho\sigma}(q) \tag{2.6}$$

are, respectively, the spin sums for $j_R=1$ and $j_R=2$. At large s, (2.4) reduce to

$$\begin{aligned} V^L\cdot V^R &= V^LV^R \text{ for } j_R=0,\\ &=-\tfrac{1}{2}(V^L)_+(V^R)_- \text{ for } j_R=1, \text{ and}\\ &=\tfrac{1}{4}(V^L)_{++}(V^R)_{--} \text{ for } j_R=2. \end{aligned} \tag{2.7}$$

A list of vertex functions is given in Table I. A symbolic coupling constant g is put in front of the vertex functions. When more than one coupling is considered, the symbols r, r', and r'' are used to denote the ratios of these other couplings to g. For example, at the $(\rho)NN$ vertex, $g=G^T$ and $r=G^V/G^T$. The couplings used are not meant to be the most general, but sufficient generality is ensured. In general, the various coupling constants can be functions of $q^2=-\tau$. Hereafter, unless otherwise stated, we shall set mesonic vertices on the left and baryonic vertices on the right.

In order to extract the Regge-cut behavior of Fig. 1, two assumptions are made. The first concerns the off-shell behavior of the Reggeon exchange. In particular, we require that this off-shell behavior must be sufficient to overcome the divergence introduced by spin complication. This is accomplished by assuming that the on-shell amplitudes of (2.2) are continued off-shell through a multiplicative softening factor G_s of the form

$$G_s=\prod_{i=1}^{4}\left(\frac{m_i{}^2-\Lambda_i{}^2}{p_i{}^2-\Lambda_i{}^2+i\epsilon}\right)^{n_i}, \tag{2.8}$$

where Λ_i are some cutoff masses. The powers n_i are determined by the degree of divergence caused by spin complication. They are listed in Table I against the corresponding vertex functions. The second assumption is the Gribov finite-mass hypothesis,[13] which states that the internal Regge amplitudes are small if the invariant mass of any of the internal lines becomes large. The finite-mass hypothesis is equivalent to demanding that (i) no internal line is allowed to have both its plus and minus components of momentum large, and (ii) all transverse momenta must not be large. In this context, a momentum component is large if it is of order $\sqrt{s}$.

The Regge amplitudes as given in Eqs. (2.1) and (2.2) display explicitly the Regge behavior, and are therefore valid only when the respective energy variables are large. But when we write down the Feynman amplitude for the RP cut corresponding to Fig. 1, the integration variables will undoubtedly run through regions for which the energy variables for the internal Regge exchanges are not large. In order to overcome this, we find it necessary in practice to make a third assumption, which will be elaborated in Sec. III.

TABLE I. List of vertex functions.

Vertex	n_1	n_3	Vertex function
$(\rho)\pi\pi$	0	0	$V^\mu = g(p_1+p_3)^\mu$
$(A_2)\pi\eta$	0	0	$V^{\mu\nu} = g(p_1+p_3)^\mu (p_1+p_3)^\nu$
$(\pi)\pi\rho$	1	1	$V = g(\epsilon_3^*)^\alpha (p_1+q)_\alpha$
$(\rho)\pi\omega$	0	0	$V_\mu = ig\epsilon_{\mu\alpha\nu\beta}(\epsilon_3^*)^\alpha q^\nu p_3^\beta$
$(B)\pi\omega$	1	1	$V_\mu = g(\epsilon_3^*)^\alpha [g_{\alpha\mu} + r(p_1+q)_\alpha (p_1+p_3)_\mu]$
$(A_2)\pi\rho$	0	0	$V^{\mu\nu} = ig\epsilon_{\alpha\beta\gamma\delta}(\epsilon_3^*)^\alpha [g^{\mu\beta}(p_1+p_3)^\nu + g^{\nu\beta}(p_1+p_3)^\mu] p_1^\gamma p_3^\delta$
$(A_2)\pi B$	1	1	$V_{\mu\nu} = g(\epsilon_3^*)^\alpha [\frac{1}{2} g_{\mu\nu}(p_1+p_3)_\nu + \frac{1}{2} g_{\nu\alpha}(p_1+p_3)_\mu + r(p_1+q)_\alpha (p_1+p_3)_\mu (p_1+p_3)_\nu]$
$(\pi)\pi f$	2	3	$V = g(t_3^*)_{\alpha\beta}(p_1+q)^\alpha (p_1+q)^\beta$
$(\rho)\pi A_2$	1	1	$V_\mu = ig\epsilon_{\mu\nu\gamma\delta}(t_3^*)_{\alpha\beta}[g^{\alpha\nu}(p_1+q)^\beta + g^{\beta\nu}(p_1+q)^\alpha] p_1^\gamma q^\delta$
$(B)\pi A_2$	2	3	$V^\mu = g(t_3^*)_{\alpha\beta}[g^{\alpha\mu}(p_1+q)^\beta + g^{\beta\mu}(p_1+q)^\alpha + r(p_1+p_3)^\mu (p_1+q)^\alpha (p_1+q)^\beta]$
$(A_2)\pi f$	1	1	$V_{\mu\nu} = ig\epsilon_{\gamma\delta\omega\tau}(t_3^*)_{\alpha\beta}[g^{\mu\gamma}(p_1+p_3)^\nu + g^{\nu\gamma}(p_1+p_3)^\mu][g^{\alpha\delta}(p_1+q)^\beta + g^{\beta\delta}(p_1+q)^\alpha] p_1^\omega (p_3-q)^\tau$
$(\pi)NN$	1	1	$V = g\bar{u}_4\gamma_5 u_2$
$(\rho)NN$	1	1	$V_\mu = g\bar{u}_4(r\gamma_\mu + i\sigma_{\mu\nu}q^\nu/2m_N)u_2$
$(B)NN$	1	1	$V_\mu = g\bar{u}_4\gamma_5(p_2+p_4)_\mu u_2$
$(A_2)NN$	1	1	$V_{\mu\nu} = g\bar{u}_4[(p_2+p_4)_\mu\gamma_\nu + (p_2+p_4)_\nu\gamma_\mu + r(p_2+p_4)_\mu (p_2+p_4)_\nu/m_N]u_2$
$(\pi)N\Delta$	2	3	$V = g\bar{\Delta}_4^\alpha q_\alpha u_2$
$(\rho)N\Delta$	2	3	$V_\mu = g\bar{\Delta}_4^\alpha\gamma_5(g_{\alpha\mu} + rp_{2\alpha}\gamma_\mu + r' p_{2\alpha}p_{2\mu})u_2$
$(B)N\Delta$	2	3	$V_\mu = g\bar{\Delta}_4^\alpha(g_{\alpha\mu} + rp_{2\alpha}\gamma_\mu + r' p_{2\alpha}p_{2\mu})u_2$
$(A_2)N\Delta$	2	3	$V_{\mu\nu} = g\bar{\Delta}_4^\alpha\gamma_5[g_{\alpha\mu}\gamma_\nu + g_{\alpha\nu}\gamma_\mu + r(g_{\alpha\mu}p_{2\nu} + g_{\alpha\nu}p_{2\mu} + r' p_{2\alpha}(p_{2\mu}\gamma_\nu + p_{2\nu}\gamma_\mu) + r'' p_{2\alpha}p_{2\mu}p_{2\nu}]u_2$

III. THE RP CUT

In extracting the large-s behavior of Fig. 1, we follow Gribov's approach,[13] treating the diagram as a Feynman graph. The Sudakov variables for the momentum k are defined as

$$\alpha = s^{-1/2}k_-, \quad \beta = s^{-1/2}k_+, \quad \vec{k} = (k_x, k_y). \tag{3.1}$$

There are 12 integration variables corresponding to the three loop momenta k_1, k, and k_2. The finite-mass hypothesis confines these variables to the following region of dominant contribution:

$$\begin{aligned} &\beta_1, \alpha_2 = O(1), \\ &\alpha_1, \beta_2, \alpha, \beta = O(m^2/s), \\ &\vec{k}, \vec{k}_1, \vec{k}_2 = O(m). \end{aligned} \tag{3.2}$$

In this region, the energy variables of the Reggeon and the Pomeranchukon exchanges are, respectively,

$$s_1 = \alpha_2\beta_1 s, \quad s_2 = (1-\alpha_2)(1-\beta_1)s, \tag{3.3}$$

and the respective submomentum transfer squares are

$$\tau_1 = \vec{k}^2, \quad \tau_2 = (\vec{q}-\vec{k})^2. \tag{3.4}$$

From (3.2) it follows that $\beta \ll \beta_1$ at the left-hand cross and $\alpha \ll \alpha_2$ at the right-hand cross, thus enabling us to factorize the two crosses within an integral over $\vec{k}$,

$$F^{(\mathrm{cut})}_{\{\lambda\}}(s,\tau) = -\tfrac{1}{2}\int \frac{d^2\vec{k}}{(2\pi)^2}\frac{e^{-A_R(m_R^2+\tau_1)}e^{-A_P\tau_2}}{m_R^2+\tau_1} \times (-is)^{\phi_R(\tau_1)+\phi_P(\tau_2)-j_R-1} N^L_{\lambda_3\lambda_1}\cdot N^R_{\lambda_4\lambda_2}, \tag{3.5}$$

where N^L and N^R are *cross structure functions* for the left- and right-hand crosses. The dot product has the same meaning as (2.7). In the following we shall concentrate on the left-hand cross, bearing in mind that N^R can be similarly treated. The explicit expression for N^L is

$$N^L_{\lambda_3\lambda_1} = s^2\int\frac{d^2\vec{k}_1}{\pi}\int_{-\infty}^{\infty}d\beta_1\int\int\frac{d\alpha_1}{2\pi i}\frac{d\alpha_3}{2\pi i}\beta_1^{\phi_R(\tau_1)-j_R}(1-\beta_1)^{\phi_P(\tau_2)}\frac{D_{\lambda_3\lambda_1}}{d_1 d_3 d_1' d_3'}\left(\frac{m_1^2-\Lambda_1^2}{d_1''}\right)^{n_1}\left(\frac{m_3^2-\Lambda_3^2}{d_3''}\right)^{n_3}, \tag{3.6}$$

where $d_i = \alpha_i \beta_1 s - \vec{k}_i^2 - m_i^2 + i\epsilon$, $i = 1, 3$, come from the hadron propagators, and

$$d_1' = (\alpha_1 s - m_1^2)(\beta_1 - 1) - \vec{k}_1^2 - m_\sigma^2 + i\epsilon,$$
$$d_3' = (\alpha_3 s - m_3^2 - \tau)(\beta_1 - 1) - (\vec{k}_3 + \vec{q})^2 - m_\sigma^2 + i\epsilon$$

are due to the σ propagators. The remaining denominators d_1'' and d_3'' are the same as d_1 and d_3 with m_i^2 replaced by Λ_i^2. We have used the variables $\alpha_3 = \alpha_1 - \alpha$ and $\vec{k}_3 = \vec{k}_1 - \vec{k}$. $D^L_{\lambda_3\lambda_1}$ are the *numerator functions* in which are lumped all factors appearing in the numerator. Rules for writing down $D^L_{\lambda_3\lambda_1}$ corresponding to a particular $V^L_{\lambda_3\lambda_1}$ are given in Appendix A.

The α_1 and α_3 integrations are easily performed by contour integration,[10] picking up poles due to the σ propagators, which are at

$$\alpha_1 s = m_1^2 - (1-\beta_1)^{-1}(\vec{k}_1^2 + m_\sigma^2),$$
$$\alpha_3 s = m_3^2 + \tau - (1-\beta_1)^{-1}[(\vec{k}_3 + \vec{q})^2 + m_\sigma^2]. \tag{3.7}$$

It turns out that both these integrals vanish unless $0 < \beta_1 < 1$, so that (3.6) can be rewritten as

$$N^L_{\lambda_3\lambda_1} = \int_0^1 d\beta_1 \beta_1^{\phi_R(\tau_1)-j_R}(1-\beta_1)^{\phi_P(\tau_2)} \mathfrak{N}^L_{\lambda_3\lambda_1}. \tag{3.8}$$

The *reduced* structure functions $\mathfrak{N}^L$ are given, after combining the remaining denominators,[11] by

$$\mathfrak{N}^L_{\lambda_3\lambda_1} = \frac{(n_1+n_3+1)!}{2\pi m_3^4 (n_1-1)!\,(n_3-1)!}\eta^{n_1+n_3} \times \int_{-1}^{1} du \int_0^{(1-u)y_1} \phi_1^{n_1-1} d\phi_1 \int_0^{(1+u)y_3} \phi_3^{n_3-1} d\phi_3 \int d^2\vec{k}_1' D^L_{\lambda_3\lambda_1}\left[\frac{\vec{k}_1'^2}{m_3^2} + \eta(A_1 + \phi_1 + \phi_3)\right]^{-(n_1+n_3+2)}, \tag{3.9}$$

where the integration variable $\vec{k}_1$ has been replaced by $\vec{k}_1'$,

$$\vec{k}_1' = \vec{k}_1 - \tfrac{1}{2}(1+u)(\vec{k} - \beta_1\vec{q}). \tag{3.10}$$

The other quantities appearing in (3.9) are

$$\eta = [(1-\beta_1)^2 m_1^2 + \beta_1 m_\sigma^2]/m_3^2, \tag{3.11}$$

$$A_1 = 1 + (1-u^2)x + (1-u)z, \tag{3.12}$$

$$x = \frac{1}{4m_3^2\eta}(\vec{k} - \beta_1\vec{q})^2, \tag{3.13}$$

$$z = \frac{1}{2m_3^2\eta}(1-\beta_1)^2(m_3^2 - m_1^2), \tag{3.14}$$

$$y_i = \frac{1}{2m_3^2\eta}(1-\beta_1)(\Lambda_i^2 - m_i^2), \quad i = 1, 3. \tag{3.15}$$

The integrations in (3.9) can be performed analytically once the numerator function D^L is explicitly written down. The process is as follows. D^L, as given by the rules of Appendix A, are expressed in terms of the Sudakov variables β_1, α_1, α_3, $\vec{k}_1$, and $\vec{k}$. The other variable β is neglected in comparison with β_1. The powers of α_1 and α_3 are then counted in order to determine the powers n_1, n_3 appearing in the softening factor G_s, and the following assignments are made:

$$n_1 = \text{highest power of } \alpha_1,$$
$$n_3 = \text{highest power of } \alpha_3. \tag{3.16}$$

Next, the values of α_1 and α_3 from (3.7) are substituted into the expression, and the variable $\vec{k}_1$ is replaced by $\vec{k}_1'$ according to (3.10), thus introducing the variable u into the expression. The final expression for D^L can be written as

$$D^L = H_0 + H_1\frac{\vec{k}_1'^2}{m_3^2} + \cdots + H_n\left(\frac{\vec{k}_1'^2}{m_3^2}\right)^n, \tag{3.17}$$

where $n \leq n_1 + n_3$, and H_i are polynomials in u to some degree m, which depends on n and i,

$$H_i = \sum_{j=0}^{m} c_{ij} u^j. \tag{3.18}$$

The coefficients c_{ij} are finite polynomials in $\vec{k}$ and $\vec{q}$. Examples of the explicit expressions for the numerator functions can be found in Appendix B. With D^L given by (3.17) and (3.18), we arrive at the final expression for $\mathfrak{N}^L$:

$$\mathfrak{N}^L = \frac{1}{2m_3^2}\sum_{i=0}^{n}\sum_{j=0}^{n} c_{ij} W_{ij}^{(n_1, n_3)}. \tag{3.19}$$

The functions $W_{ij}^{(n_1, n_3)}$ are given in Appendix C. It is noted that the $W_{ij}^{(n_1, n_3)}$ functions at a particular vertex do not depend on the spins of the external particles or the type of exchanged Reggeon. The external spins and the Reggeon coupling serve only to determine the values of n_1 and n_3.

The calculation of the right-hand cross is identical to that of the left-hand cross. In going from the N^L to N^R, we merely have to make the substitution

$$(m_1, m_3; \beta_1, \alpha_1, \vec{k}_1; \alpha, \vec{k}; \vec{q}) \rightarrow (m_2, m_4; \alpha_2, \beta_2, -\vec{k}_2; -\beta, \vec{k}; \vec{q}). \tag{3.20}$$

Equation (3.8), for example, will be replaced by a similar expression with an integral over the variable α_2.

In practical evaluation of the β_1 and α_2 integrations, we require a third assumption in the model. The assumption is that when a hadron emits a σ particle, its large component of momentum (p_{1+} on

the left and p_{2-} on the right) must be *shared equally* by the emitted σ and the virtual hadron. Since by definition $k_{1+}=\beta_1 p_{1+}$, and $k_{2-}=\alpha_2 p_{2-}$, this assumption is equivalent to setting $\beta_1=\alpha_2=\frac{1}{2}$. The purpose of the assumption is to avoid the unwanted and artificial divergences in the β_1 and α_2 integrations, which arise from the singularities at the end points $\beta_1, \alpha_2=0, 1$. The singularities are artificial because at these end-point regions one of the two energy variables s_1 and s_2 is not large enough to justify use of the Regge form (2.1) or (2.2) for the internal exchange. To be exact, we must modify the internal exchanges appropriately at low energies. But since we are concerned only with extracting the Regge-cut behavior from the Mandelstam diagram, we shall avoid these end-point regions. This is most effectively taken care of by the third assumption. With the help of the last assumption, we can rewrite (3.5) as

$$F_{\{\lambda\}}^{(\mathrm{cut})}(s,\tau)=-\tfrac{1}{8}\int\frac{d^2\vec{k}}{(2\pi)^2}\frac{e^{-\lambda_R(m_R{}^2+\tau_1)}e^{-\lambda_P\tau_2}}{m_R{}^2+\tau_1}K_{\{\lambda\}}, \tag{3.21}$$

where

$$\lambda_{R,P}=A_{R,P}+\phi'_{R,P}\left(\ln\frac{s}{4}-i\frac{\pi}{2}\right), \tag{3.22}$$

$$K_{\{\lambda\}}=\mathfrak{N}^L_{\lambda_3\lambda_1}\cdot\mathfrak{N}^R_{\lambda_4\lambda_2}. \tag{3.23}$$

It is understood that in (3.23) the variables β_1 and α_2 have been set equal to $\frac{1}{2}$.

We reiterate here the main steps involved in the calculation of the RP cut in a particular reaction from the diagram model:

1. Write down the vertex functions for the Reggeon exchange.
2. Write down the corresponding cross numerator functions according to Appendix A.
3. Express the numerator functions in terms of Sudakov variables, assign values to n_1, n_2, n_3, and n_4, and bring the numerator functions into the forms (3.17) and (3.18).
4. Compute the W_{ij} functions according to Appendix C.
5. Obtain the cut amplitudes from (3.19) and (3.21).

IV. SOME GENERAL FEATURES OF THE STRUCTURE FUNCTIONS

The most prominent characteristic of the diagram model lies in the factor $K_{\{\lambda\}}$ which appears in the final expression (3.21) for the cut. In comparison, if we were to generate the RP cut via absorptive corrections,[6] using the same Regge exchanges (2.1) and (2.2) as inputs, we would obtain an expression similar to (3.21), but with

$$\lambda_{R,P}^{(\mathrm{abs})}=A_{R,P}+\phi'_{R,P}\left(\ln s-i\frac{\pi}{2}\right) \tag{4.1}$$

and

$$K_{\{\lambda\}}^{(\mathrm{abs})}=\gamma_P{}^2B_{\{\lambda\}}\cos n\theta, \tag{4.2}$$

where θ is the angle between the vectors $\vec{q}$ and $\vec{k}$, n is the net helicity flip, and the residue function $B_{\{\lambda\}}$ is to be evaluated with $\tau\to\tau_1$. It is obvious from (4.2) that, besides the factor $\cos n\theta$, the structure of the cut comes entirely from the Reggeon couplings. If a more complex structure were desired of the cut, one would have to employ a Pomeranchukon with complicated structure. The diagram model, on the other hand, generates the cut with a structure given by the factor $K_{\{\lambda\}}$ which, in this model, is the product of two structure functions corresponding to the two crosses. Each cross structure function contains the detailed information about the cross, including the helicity structure. As given by (3.19), two factors come into the structure function, (i) W_{ij} which are due to the inherent cross structure, and (ii) c_{ij} which describes the helicity structure of the cross.

The W_{ij} functions come from the four propagator denominators at the cross and, as such, they are an inherent feature of the cross. They do not depend on external spins or on Reggeon coupling, except for assigning values to n_1 and n_3. Calculation of such functions is outlined in Appendix C. In general, they are given by logarithmic functions of complicated arguments. The dependence of W_{ij} on the momenta $\vec{k}$ and $\vec{q}$ is simple, and it is through the variable

$$\tau'=(\vec{k}-\tfrac{1}{2}\vec{q})^2. \tag{4.3}$$

It is interesting to note that, with the third assumption of the model, the W_{ij} on the left and those on the right are functions of this same variable τ'. This is a reflection of the left-right symmetry inherent in the model. In fact, if the two crosses are identical, a relation between the structure functions exists. For example, when both crosses are NN crosses, we have the relation

$$N^L_{\lambda\mu}=\eta_R N^R_{-\lambda-\mu}$$

where η_R is the naturality of the Reggeon ($\eta_R=+1$ for a Reggeon with natural parity, $\eta_R=-1$ for a Reggeon with unnatural parity). The τ' dependence of W_{ij} is illustrated in Fig. 2. It is observed that the dependence is typical of all W_{ij}; it is monotonically and gently decreasing. The W_{ij} also depend on the σ mass m_σ and the two cutoff masses Λ_1 and Λ_3. The dependence on m_σ, Λ_1, and Λ_3 is best illustrated in the case of the $\pi\rho$ cross, i.e., the cross at the $\pi\rho$ vertex. The behavior of $W_{ij}^{(1,1)}$ at $\tau'=0$ is such that for $m_1{}^2, m_3{}^2\ll m_\sigma{}^2\ll\Lambda_1{}^2, \Lambda_3{}^2$,

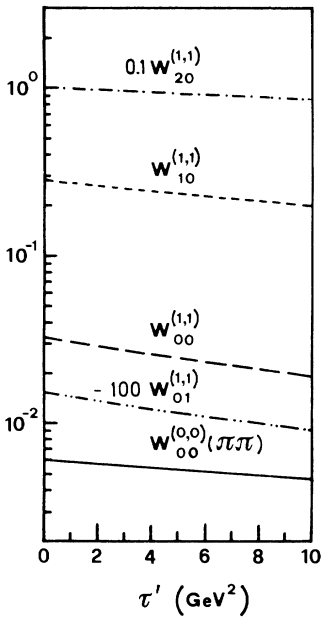

FIG. 2. Dependence of W_{ij} on $\tau' = (\vec{k} - \frac{1}{2}\vec{q})^2$ at $m_\sigma{}^2 = 13$ GeV^2 and $\omega = \Lambda_1{}^2 - m_1{}^2 = \Lambda_3{}^2 - m_3{}^2 = 20$ GeV^2 for the $\pi\rho$ cross. $W_{00}^{(0,0)}$ refers to the $\pi\pi$ cross.

$$W_{00}, W_{02}, W_{04} \sim m_3{}^2/m_\sigma{}^2,$$
$$W_{01}, W_{03} \sim m_3{}^2(m_3{}^2 - m_1{}^2)/m_\sigma{}^4,$$
$$W_{10}, W_{12} \sim \ln(\Lambda^2/m_\sigma{}^2),$$
$$W_{11} \sim (m_3{}^2 - m_1{}^2)/m_\sigma{}^2,$$
$$W_{20} \sim \Lambda^2/m_3{}^2.$$

This is illustrated in Figs. 3 and 4. We find that in general W_{ij} are decreasing functions of $m_\sigma{}^2$, but are increasing functions of Λ^2.

The c_{ij} functions come from the numerator functions and, therefore, depend strongly on the external spins as well as the Reggeon coupling. The helicity structure of the cross structure function is reflected in c_{ij} via the following pattern:

1. For $\lambda_3 - \lambda_1 = 0$,

$$c_{ij} = a_1 + a_2 k^{(+)} q^{(-)} + a_3 k^{(-)} q^{(+)} + a_4 (k^{(+)} q^{(-)})^2 + a_5 (k^{(-)} q^{(+)})^2 + \cdots,$$

where the a_i are, in general, polynomials in $\vec{k}^2$ and $\vec{q}^{\,2}$.

2. For $\lambda_3 - \lambda_1 = 1$,

$$c_{ij} = a_1' k^{(-)} + a_2' q^{(-)} + a_3' k^{(-)} k^{(-)} q^{(+)} + a_4' q^{(-)} q^{(-)} k^{(+)} + \cdots.$$

3. For $\lambda_3 - \lambda_1 = 2$,

$$c_{ij} = a_1'' k^{(-)} k^{(-)} + a_2'' q^{(-)} k^{(-)} + a_3'' q^{(-)} q^{(-)} + \cdots$$

In the above, the symbol $k^{(\pm)}$ is used to denote k_x

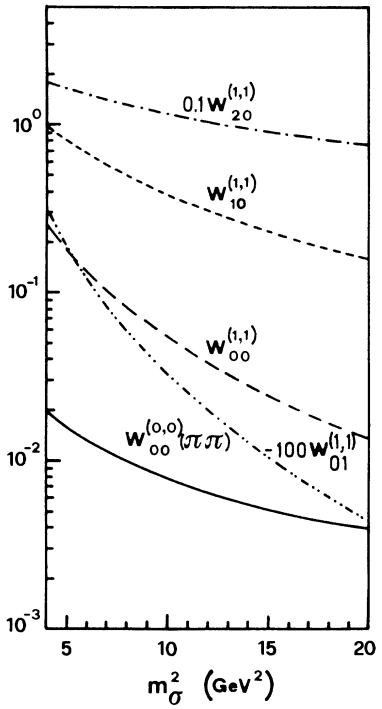

FIG. 3. Dependence of $W_{ij}(\tau' = 0)$ on $m_\sigma{}^2$ at $\omega = \Lambda_1{}^2 - m_1{}^2 = \Lambda_3{}^2 - m_3{}^2 = 20$ GeV^2, for $\pi\rho$ cross. $W_{00}^{(0,0)}$ refers to the $\pi\pi$ cross.

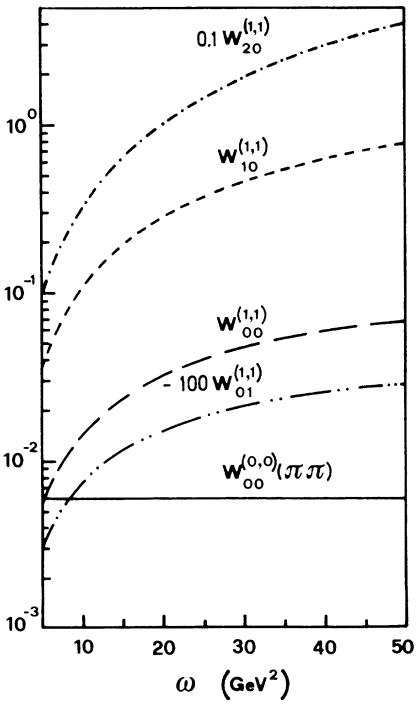

FIG. 4. Dependence of $W_{ij}(\tau' = 0)$ on $\omega = \Lambda_1{}^2 - m_1{}^2 = \Lambda_3{}^2 - m_3{}^2$ at $m_\sigma{}^2 = 13$ GeV^2 for the $\pi\rho$ cross. $W_{00}^{(0,0)}$ refers to the $\pi\pi$ cross.

$\pm ik_y$. We have, of course, $q^{(+)}=q^{(-)}=q_x=-\sqrt{\tau}$, since $q_y=0$. The pattern can be understood if we identify $k^{(-)}$ and $q^{(-)}$ as objects which raise the helicity by one unit at the left-hand cross, and $k^{(+)}$ and $q^{(+)}$ as objects which lower the helicity by one unit. Then for $\lambda_3-\lambda_1=0$ the structure of c_{ij} is such that there are equal numbers of (+) and (−) objects in each term. For $\lambda_3-\lambda_1=1$ there is an excess of one (−) object in each term, and for $\lambda_3-\lambda_1=2$ there are two excessive (−) objects in each term. The roles of (+) and (−) objects are interchanged at the right-hand cross.

The quantum numbers of the RP cut are essentially the same as those of the Reggeon except for parity. We can, nevertheless, form combinations of the cross structure functions which project out definite parity. Referring to the left-hand cross, the combination with naturality η is

$$N^{(\eta)}_{\lambda_3\lambda_1}=N_{\lambda_3\lambda_1}+\eta\eta_1\eta_3(-1)^{\lambda_3-\lambda_1}N_{-\lambda_3-\lambda_1}, \tag{4.4}$$

where η_1 and η_3 are naturalities of particles 1 and 3, respectively. In a similar way, when particles 1 and 3 are identical, combinations can be formed that have definite C parity; the combination with C naturality η^C is

$${}^{(\eta^C)}N_{\lambda_3\lambda_1}=N_{\lambda_3\lambda_1}+\eta^C N_{-\lambda_1-\lambda_3}. \tag{4.5}$$

Of the vertices considered, only the NN vertex is relevant to C conjugation. Combinations with definite η and η^C are shown in Table II. It is noticed that only the combination $N_{1/2,1/2}-N_{-1/2-1/2}$ has unnatural C parity, and it receives no contribution from our RP cuts. This is obvious because, since we do not consider A_1-type Regge poles, the contributions of RP cut to unnatural C parity must necessarily be absent.

One useful property of the structure functions is the relation

$$N_{\lambda_3\lambda_1}=\eta_R\eta_1\eta_3(-1)^{\lambda_3-\lambda_1}N^{*}_{-\lambda_3-\lambda_1}, \tag{4.6}$$

where η_R is the naturality of the Reggeon. This relation is important because, together with (4.4), it implies that the real part of a structure function always has naturality $\eta=\eta_R$, whereas the imaginary part has naturality $\eta=-\eta_R$. It is found that the structure functions are such that $\mathrm{Im}N$ is proportional to k_y and is an odd function of k_y, whereas $\mathrm{Re}N$ is an even function of k_y. This implies that the cut contributes to amplitudes of naturality $\eta=-\eta_R$ with a factor k_y^2 in $K_{\{\lambda\}}$, but the contributions to amplitudes of naturality $\eta=\eta_R$ need not contain any factor of k_y. Cut contributions with a factor of k_y from one cross and no factor of k_y from the other cross are zero because they are of mixed naturalities, and are strictly forbidden by parity conservation; parity must be conserved from one cross to another, although the cut itself has no definite parity.

TABLE II. Combinations of the NN cross structure functions exhibiting definite naturality η and C naturality η^C.

Structure function	η	η^C
$N_{1/2,1/2}+N_{-1/2-1/2}$	+	+
$N_{1/2,1/2}-N_{-1/2-1/2}$	−	−
$N_{1/2-1/2}+N_{-1/2,1/2}$	−	+
$N_{1/2-1/2}-N_{-1/2,1/2}$	+	+

At a mesonic vertex, the structure function N_{00} is constrained by (4.6) to be either real or imaginary. It is purely imaginary when $\eta_R=-\eta_1\eta_3$. In this case, it is suppressed by the factor q_xk_y. One should note that N_{00}, since it is helicity nonflip, need not contain any factor of q_x. The presence of the suppressing factor is due entirely to N_{00} having naturality opposite to that of the Reggeon. This suppression is observed at the following vertices: $(\rho)\pi\omega$, $(A_2)\pi\rho$, $(\rho)\pi A_2$, and $(A_2)\pi f$. On the other hand, when $\eta_R=\eta_1\eta_3$, N_{00} is real and is enhanced. There is a similar suppression in the structure function $N_{1/2,1/2}$ at a baryonic vertex. For the NN vertex, either $\mathrm{Re}N_{1/2,1/2}$ or $\mathrm{Im}N_{1/2,1/2}$ has unnaturality C parity. $\mathrm{Re}N_{1/2,1/2}$ will be of unnatural C parity when $\eta_R=-$, in which case $\mathrm{Im}N_{1/2,1/2}$ is suppressed by the same factor q_xk_y. It therefore follows that the contributions of πP and BP cuts are unimportant in $N_{1/2,1/2}$ at the NN vertex. On the other hand, when $\eta_R=+$, $\mathrm{Im}N_{1/2,1/2}$ is of unnatural C parity and $\mathrm{Re}N_{1/2,1/2}$ is enhanced. For the $N\Delta$ vertex, $\mathrm{Im}N_{1/2,1/2}$ is similarly suppressed, while $\mathrm{Re}N_{1/2,1/2}$ is always enhanced. The above suppression scheme leads to strong suppression in the cut contributions to amplitudes of naturality opposite to the Reggeon and which do not partake in the $M=1$ conspiracy.

There is a *second* suppression scheme which is operative only at very high energies.[14,15] This suppression is particularly important in structure functions where there is a change of helicity by one unit. Structure functions with naturality opposite to η_R are suppressed in comparison with structure functions with naturality $-\eta_R$. The suppression is directly related to the quantity $m_R^2\ln s$, and therefore grows logarithmically as s increases. However, the πP cut, owing to the smallness of the pion mass, is little affected by this suppression scheme. This has important consequences on conspiracy.

V. CHARACTERISTICS OF THE *RP* CUTS

The RP cuts from this model, besides being richer in structure, are also capable of contributing to all amplitudes, except those which have unnatural C parity. We therefore find the cut to populate in more amplitudes than does an absorptive cut. For example, our πP cut contributes to four of the five amplitudes in np CEX, whereas the absorptive cut contributes only to two of them, namely $F_{1/2,1/2;-1/2-1/2} \pm F_{1/2-1/2;-1/2,1/2}$. The extra amplitudes receiving contributions from our πP cut are $F_{1/2,1/2;1/2,1/2} + F_{1/2,1/2;-1/2-1/2}$ and $F_{1/2,1/2;1/2-1/2}$. In ρ production, our πP cut has an extra contribution in $F_{1,1/2;0,1/2} + F_{-1,1/2;0,1/2}$. In ω production, the extra contribution of the ρP cut goes to $F_{0,1/2;0-1/2}$. It is observed that all these extra amplitudes which receive cut contributions only in this model have naturality opposite to the Reggeon. They are all suppressed to some degree because of the first suppression scheme mentioned in Sec. IV. It therefore appears that although the cut has extra contributions, these extra contributions are suppressed. They are, nevertheless, of importance. For example, because of its extra contribution in $F_{0\,1/2;0-1/2}$, the ρP cut has a small contribution to the density matrix element ρ_{00}^H in ω production.

All RP cuts are found to be self-conspiratorial with respect to the $M=1$ conspiracy relation. We recall that the $M=1$ conspiracy relation is a consequence of angular momentum conservation; it relates amplitudes of both naturalities which have a unit helicity flip at each vertex. For example, the conspiracy relation for vector-meson production is

$$(F_{1,1/2;0-1/2} + F_{-1,1/2;0-1/2}) - (F_{1,1/2;0-1/2} - F_{-1,1/2;0-1/2}) = 0, \tag{5.1}$$

at $\tau = 0$. In order to have a conspiratorial solution, this relation must be satisfied nontrivially. The criterion is $F_{1,1/2;0-1/2}(\tau = 0) \neq 0$. This is satisfied by all RP cuts in this model. Self-conspiracy is an important feature of Regge cuts. In π-exchange processes, for example, it is the conspiratorial πP cut interfering with an evasive π pole that accounts for the sharp forward spikes observed in np CEX, π^+ photoproduction, and $\rho_{11}^H d\sigma/dt$ of ρ^0 production.[10,11] For other RP cuts, this conspiratorial feature of the cut is masked by the second suppression scheme discussed in Sec. IV. Contribution to the amplitude $F_{1,1/2;0-1/2} - \eta_R F_{-1,1/2;0-1/2}$, which has naturality $-\eta_R$, is suppressed at large s, resulting in the suppression also of the contribution to $F_{1,1/2;0-1/2} + \eta_R F_{-1,1/2;0-1/2}$ at $\tau = 0$. The cut therefore appears to be evasive, with a small residual conspiratorial effect because the contribution to $F_{1,1/2;0-1/2}$ at $\tau = 0$ is not strictly vanishing. The degree of evasiveness increases logarithmically as s increases. But at lower energies, particularly at $s < 30$ GeV^2, the suppression is weak, and we expect that the conspiratorial effect of the RP cuts be visible, for example, in B^0 production.

At very high energies, the last integration over $\vec{k}$ in the expression (3.21) for the cut amplitudes can be evaluated approximately. This is achieved by expanding $K_{\{\lambda\}}$ into a Taylor series in $\vec{k}$,

$$K_{\{\lambda\}} = \sum_{ij} a_{ij} k_x^i k_y^j, \tag{5.2}$$

and evaluating the following integrals:

$$I_{ij} = \int \frac{d^2\vec{k}}{(2\pi)^2} \frac{e^{-\lambda_R(m_R^2+\tau_1)} e^{-\lambda_P \tau_2}}{m_R^2 + \tau_1} k_x^i k_y^j. \tag{5.3}$$

With the help of I_{ij}, (3.21) becomes

$$F_{\{\lambda\}}^{(\mathrm{cut})}(s,\tau) = -\tfrac{1}{8} \sum_{ij} a_{ij} I_{ij}. \tag{5.4}$$

The integral I_{00} is given by

$$I_{00} = \frac{1}{4\pi} e^{-\lambda_R m_R^2} e^{-\lambda_R \lambda_P \tau/(\lambda_R+\lambda_P)} \frac{G(z,x)}{z}, \tag{5.5}$$

where

$$z = (\lambda_R + \lambda_P) m_R^2, \tag{5.6}$$

$$x = \left(\frac{\lambda_P}{\lambda_R+\lambda_P}\right)^2 \frac{\tau}{m_R^2}, \tag{5.7}$$

and $G(z,x)$ is a descending series in z,

$$G(z,x) = \sum_{n=0}^{\infty} \frac{(-1)^n}{n!} \frac{1}{z^n} \left(\frac{d}{dx}\right)^n x^n \left(\frac{d}{dx}\right)^n \frac{x^n}{1+x}. \tag{5.8}$$

In arriving at the expression (5.5) for I_{00} and the series expansion for G, we have already assumed that $z \gg 1$ and $|x| < 1$. The condition $z \gg 1$ is realized by most RP cuts, except the πP cut, at $s \gg 30$ GeV^2. For the πP cut, $z \gg 1$ can be fulfilled only at $s \gg 10^{23}$ GeV^2. It therefore appears that (5.5) is not good for the πP cut. We shall return to this point shortly. Assuming that (5.5) and (5.8) are valid expressions, we can express the other I_{ij} in terms of I_{00}, for example,

$$I_{10} = -m_R \sqrt{x} \left(1 + \frac{1}{zG} \frac{\partial G}{\partial x}\right) I_{00}, \tag{5.9}$$

$$I_{20} = m_R^2 \left(x + \frac{1}{2z} + \frac{2x}{zG} \frac{\partial G}{\partial x} + \frac{1}{2z^2 G} \frac{\partial G}{\partial x} + \frac{x^2}{z^2 G} \frac{\partial^2 G}{\partial x^2}\right) I_{00}, \tag{5.10}$$

$$I_{02} = \frac{1}{2z} m_R^2 \left(1 + \frac{1}{zG} \frac{\partial G}{\partial x}\right) I_{00}. \tag{5.11}$$

In the limit $z \gg 1$, we can approximate G by

$$G(z,x)\approx(1+x)^{-1}. \tag{5.12}$$

In this limit,

$$I_{ij}\approx\left(\frac{\lambda_P}{\lambda_R+\lambda_P}q_x\right)^i\delta_{j0}I_{00}, \tag{5.13}$$

so that (5.4) becomes, after resumming the Taylor series,

$$F^{(\mathrm{cut})}_{\{\lambda\}}(s,\tau)\approx-\tfrac{1}{8}I_{00}K_{\{\lambda\}}\left(\vec{k}\to\frac{\lambda_P}{\lambda_R+\lambda_P}\vec{q}\right). \tag{5.14}$$

We recall that $K_{\{\lambda\}}$ is the product of the two structure functions. From the exact formula (3.21), the cut has factorization within the $\vec{k}$ integration. But Eq. (5.14) tells us that in the limit $z\to\infty$, cut amplitudes factorize completely. This quasifactorization of the cut is accompanied by the second suppression scheme of Sec. IV. It is important to note that this quasifactorization is not valid for the πP cut.

To see how the second suppression scheme of Sec. IV operates, we recall that the opposite-naturality contribution of the cut, i.e., the contribution to amplitudes with naturality opposite to η_R, has an extra factor of k_y^2 in $K_{\{\lambda\}}$. In amplitudes with a unit helicity flip at both sides, which are the relevant amplitudes for $M=1$ conspiracy, the ratio of the opposite-naturality contribution to the like-naturality contribution is roughly given by the ratio of I_{02} to I_{20}, which, when $z\gg1$, is

$$I_{02}/I_{20}\approx1\Big/\left[2xz+\frac{1-4x-x^2}{(1+x)^2}\right]. \tag{5.15}$$

Therefore, the opposite-naturality contributions are suppressed when $z\gg1$; the suppression increases logarithmically as s increases, and almost linearly as τ increases. At $\tau=0$ the unsuppressed like-naturality contribution of the cut is forced by the conspiracy relation (5.1) to suppress itself, giving rise to a forward dip structure to the like-naturality contribution. The stronger the suppression, the more profound is the forward dip, thus rendering the cut to appear evasive.

The πP cut is an exception by itself. Because of the smallness of the pion mass, the quantity z is not large at energies which are within reach. We, therefore, cannot express I_{00} by (5.5). It can, nevertheless, be demonstrated that I_{00} is well approximated, at least for $\tau<10m_\pi^2$, by the formula

$$I_{00}\approx\mathfrak{a}e^{-\lambda\tau}. \tag{5.16}$$

From (5.16) we can derive expressions for other I_{ij} in terms of I_{00}, similar to Eqs. (5.9) to (5.11). It is found that there is little suppression of opposite-naturality contributions. As a result, the conspiratorial effect of the πP cut is very prominent.

Another important characteristic of the RP cuts generated in this model concerns pole-cut interference. Contrary to the absorption model, we find that the pole-cut interference is not necessarily destructive. Examples of constructive interference are found in (i) the πP cut with π pole in the amplitude $F_{0,1/2;0,-1/2}$ for ρ^0 production,[11] and (ii) the ρP cut with ρ pole in ω^0 production. In some cases the interference depends on the parameter m_0^2. A detailed analysis of the pole-cut interference will be presented elsewhere.

VI. CONCLUSION

We have presented an alternative model for calculating Reggeon-Pomeranchukon cuts. The model is simple and easily applicable. Spin complication is treated in a natural way. In practical application, the calculation of the cut involves essentially two steps: (i) calculation of the numerator functions D^L and D^R, and (ii) evaluation of the appropriate W_{ij} functions. One can actually evaluate all the W_{ij} functions for all types of RP cuts and list them as known functions. Only the numerator functions need then to be calculated in any particular case.

The diagram model is found to give structures to the cut even with a simple Pomeranchukon. In addition, the cut contributes to more s-channel helicity amplitudes than does the absorptive cut. All the contributions from a cut are characterized by one *strength*, which is the product of two cross coupling constants as defined by (A6). The relative strengths of the various contributions are inherent in the model. It is found that cut contributions to amplitudes with naturality opposite to the Reggeon are somewhat suppressed. Those opposite-naturality contributions which do not take part in the $M=1$ conspiracy are strongly suppressed. Those which partake in the $M=1$ conspiracy are suppressed at very high energies, except for the case of the πP cut.

All RP cuts are found to be self-conspiratorial. This self-conspiracy is particularly prominent in the πP cut, which results in the sharp forward spikes observed in π exchange processes. For the other RP cuts, the conspiratorial effect is masked by the suppression of the opposite-naturality contribution at high energies. However, the effect may be visible in B^0 production at $s<30$ GeV^2. At very high energies, the RP cut (except the πP cut) exhibits quasifactorization, a property not observed at lower energies.

ACKNOWLEDGMENTS

The author wishes to thank Professor Abdus Salam, the International Atomic Energy Agency,

and UNESCO for hospitality at the International Centre for Theoretical Physics, Trieste.

APPENDIX A

In this appendix we give the rules for writing down the cross numerator function. In Table I, the vertex functions fall into five classes, i.e., πP ($P=\pi,\eta$), πV ($V=\rho,\omega,B$), πT ($T=f,A_2$), NN, and $N\Delta$. The rules are written separately for each of the classes. Lorentz indices on the vertex functions and the numerator functions are abbreviated by the letter A:

1. πP vertex:
$$V^A=g\Gamma^A(p_1,p_3),\qquad D^A=g_C\Gamma^A(k_1,k_3), \tag{A1}$$

2. πV vertex:
$$V^A=g(\epsilon_3^*)^\alpha\Gamma^A{}_\alpha(p_1,p_3),$$
$$D^A=g_C(\epsilon_3^*)_\sigma(-g^{\sigma\alpha}+k_3^\sigma k_3^\alpha/m_3{}^2)\Gamma^A{}_\alpha(k_1,k_3), \tag{A2}$$

3. πT vertex:
$$V^A=g(t_3^*)_{\alpha\beta}\Gamma^{A\alpha\beta}(p_1,p_3),\qquad D^A=g_C(t_3^*)^{\rho\sigma}\Sigma_{\rho\sigma\alpha\beta}(k_3)\Gamma^{A\alpha\beta}(k_1,k_3), \tag{A3}$$

where $\Sigma_{\rho\sigma\alpha\beta}$ is as given in (2.6), with m_R replaced by m_3,

4. NN vertex:
$$V^A=g\bar u_4\Gamma^A(p_2,p_4)u_2,\qquad D^A=g_C\bar u_4(\not k_4+m_N)\Gamma(k_2,k_4)(\not k_2+m_N)u_2, \tag{A4}$$

5. $N\Delta$ vertex:
$$V^A=g\bar\Delta_4{}^\alpha\Gamma^A{}_\alpha(p_2,p_4)u_2,$$
$$D^A=g_C\bar\Delta_4{}^\beta(-g_{\alpha\beta}+\tfrac{2}{3}k_{4\alpha}k_{4\beta}/m_\Delta{}^2+\tfrac{1}{3}k_{4\alpha}\gamma_\beta/m_\Delta)\times(\not k_4+m_\Delta)\Gamma^{A\alpha}(k_2,k_4)(\not k_2+m_N)u_2. \tag{A5}$$

In the expressions for D^A, we have lumped all the coupling constants into one single quantity g_C, which we shall call the cross coupling constant,

$$g_C=\gamma_P g f_1 f_3/(16\pi^2), \tag{A6}$$

where f_1 and f_3 are coupling constants of the σ particle to particles 1 and 3, respectively.

APPENDIX B

We give here the explicit expressions for some of the numerator functions:

1. $(\pi)\pi\rho$ cross:
$$D_{00}^L=-\frac{1}{2m_3{}^3}\{4\vec{k}_1'^4+(m_3{}^2-m_1{}^2+6m_\sigma{}^2+4u\vec{k}'^2-\vec{k}^2)\vec{k}_1'^2+[\tfrac{1}{2}m_1{}^2+m_3{}^2-m_\sigma{}^2+\vec{k}^2-\tfrac{1}{2}(1+u)^2\vec{k}'^2][\tfrac{1}{2}m_3{}^2-2m_\sigma{}^2-\tfrac{1}{2}(1-u)^2\vec{k}'^2]\},$$
$$D_{10}^L=\frac{1}{\sqrt{2}m_3{}^2}\{[2u\vec{k}_1'^2+\tfrac{1}{2}(3+u)m_3{}^2]k'^{(-)}+m_3{}^2q^{(-)}+\tfrac{1}{2}(1-u)[\tfrac{1}{2}m_1{}^2-m_\sigma{}^2+\vec{k}^2-\tfrac{1}{2}(1+u)^2\vec{k}'^2]k'^{(-)}\},$$

where $\vec{k}'=\vec{k}-\frac{1}{2}\vec{q}$, and the symbol $k^{(\pm)}$ denotes $k_x\pm ik_y$.

2. $(\rho)\pi\omega$ cross:
$$(D_{00}^L)_+=\frac{1}{8m_3}\sqrt{s}(1-u)(q^{(+)}k^{(-)}-q^{(-)}k^{(+)}),$$
$$(D_{10}^L)_+=\frac{1}{2\sqrt{2}}\sqrt{s}\,k'^{(-)}.$$

3. $(\pi)NN$ cross:
$$D^R_{1/2,1/2}=-\tfrac{3}{8}(q^{(+)}k^{(-)}-q^{(-)}k^{(+)}),$$
$$D^R_{1/2,-1/2}=\frac{1}{2m_N}\{[2m_\sigma{}^2-\tfrac{7}{2}m_N{}^2+\tfrac{1}{2}(1-u^2)(\vec{k}'^2-\tfrac{1}{2}q^{(-)}k'^{(+)})]k'^{(+)}-\tfrac{9}{4}m_N{}^2q^{(+)}\}.$$

4. $(\rho)NN$ cross:
$$D^R_{1/2,1/2}=\frac{\sqrt{s}}{m_N}\{\gamma\vec{k}_2'^2+\tfrac{1}{4}\gamma[9m_N{}^2-(1-u^2)\vec{k}'^2]-\tfrac{3}{4}\vec{k}\cdot\vec{k}'\},$$
$$D^R_{1/2,-1/2}=-\frac{\sqrt{s}}{m_N{}^2}\{\tfrac{3}{2}(\gamma+\tfrac{3}{4})m_N{}^2k'^{(+)}+\tfrac{9}{16}m_N{}^2q^{(+)}-\tfrac{1}{8}(1-u^2)[(\vec{k}^2-\tfrac{1}{4}\vec{q}^2)k'^{(+)}-\tfrac{1}{2}\vec{k}'^2q^{(+)}]\}.$$

APPENDIX C

The W_{ij} functions are defined by

$$W_{ij}^{(n_1,n_3)}=\int_{-1}^{1}du\,u^jL_i^{(n_1,n_3)}, \tag{C1}$$

where

$$L_i^{(n_1,n_3)}=\frac{i!\,(n_1+n_3-i)!}{(n_1-1)!\,(n_3-1)!}\eta^{i-1}\int_0^{(1-u)y_1}\phi_1^{n_1-1}d\phi_1\int_0^{(1+u)y_3}\phi_3^{n_3-1}d\phi_3(A_1+\phi_1+\phi_3)^{-(n_1+n_3-i+1)}, \tag{C2}$$

for $n_1, n_3 \geq 1$, and

$$L_0^{(0,0)}=\frac{1}{\eta}A_1^{-1}. \tag{C3}$$

The L_i functions satisfy the following relation:

$$L_{m-1}^{(n_1,n_3)}=-\frac{1}{m\eta}\frac{d}{dA_1}L_m^{(n_1,n_3)}, \tag{C4}$$

so that once $L_{n_1+n_3}^{(n_1,n_3)}$ is known, all the other L_i can be calculated. We give here the functions $L_{n_1+n_3}^{(n_1,n_3)}$ for the two important cases (i) $n_1=n_3=1$ and (ii) $n_1=2$, $n_3=3$:

$$L_2^{(1,1)}=2\eta(A_4\ln A_4-A_3\ln A_3-A_2\ln A_2+A_1\ln A_1), \tag{C5}$$

$$\begin{aligned}L_5^{(2,3)}=-5\eta^4\{&[(A_4^4\ln A_4-A_3^4\ln A_3-A_2^4\ln A_2+A_1^4\ln A_1)-(\tfrac{1}{2}+\tfrac{1}{3}+\tfrac{1}{4})(A_4^4-A_3^4-A_2^4+A_1^4)]\\&-4\delta_1[(A_4^3\ln A_4-A_2^3\ln A_2)-(\tfrac{1}{2}+\tfrac{1}{3})(A_4^3-A_2^3)]\\&-4\delta_3[(A_4^3\ln A_4-A_3^3\ln A_3)-(\tfrac{1}{2}+\tfrac{1}{3})(A_4^3-A_3^3)]\\&+6\delta_3{}^2[(A_4^2\ln A_4-A_3^2\ln A_3)-\tfrac{1}{2}(A_4^2-A_3^2)]\\&+12\delta_1\delta_3(A_4^2\ln A_4-\tfrac{1}{2}A_4^2)-12\delta_1\delta_3{}^2A_4\ln A_4\},\end{aligned} \tag{C6}$$

where

$$\delta_{1,3}=(1\mp u)y_{1,3}, \tag{C7}$$

A_1 is given by (3.12), and

$$\begin{aligned}A_2&=A_1+\delta_1,\\A_3&=A_1+\delta_3,\\A_4&=A_1+\delta_1+\delta_3.\end{aligned} \tag{C8}$$

The computation of W_{ij} from L_i is straightforward but tedious, and will not be given here. We give here only the simplest of all W_{ij}, i.e., $W_{00}^{(0,0)}$ for the case $m_1=m_3$:

$$W_{00}^{(0,0)}=\frac{1}{\eta[x(1+x)]^{1/2}}\ln\left[\frac{(1+x)^{1/2}+\sqrt{x}}{(1+x)^{1/2}-\sqrt{x}}\right], \tag{C9}$$

where η and x are as given by (3.11) and (3.13), respectively. The general W_{ij} have more complicated structure than (C9). But they all have one feature in common, namely the dependence on the logarithmic function

$$Z_n(a)=a^{-(2n+1)}\left[\ln\frac{1+a}{1-a}-2\left(a+\tfrac{1}{3}a^3+\cdots+\frac{1}{2n-1}a^{2n-1}\right)\right], \tag{C10}$$

where a is some algebraic function of x, z, y_1, and y_3. It should be noted that when particles 1 and 3 are identical, $m_1=m_3$, $y_1=y_3$, and L_i are even functions of u. This implies that $W_{ij}=0$ unless j is even.

*On leave of absence from Physics Department, University of Malaya, Kuala Lumpur, Malaysia.

[1]R. J. N. Phillips, Nucl. Phys. B2, 394 (1967).
[2]F. Arbab and J. W. Dash, Phys. Rev. 163, 1603 (1967).
[3]J. Ball, W. Frazer, and M. Jacob, Phys. Rev. Lett. 20, 518 (1968).
[4]M. LeBellac, Phys. Lett. 25B, 524 (1967).
[5]Aachen-Berlin-CERN collaboration, Phys. Lett. 27B, 174 (1968); Nucl. Phys. B8, 45 (1968).
[6]F. Henyey, G. L. Kane, J. Pumplin, and M. H. Ross, Phys. Rev. 182, 1579 (1969).
[7]B. J. Hartley and G. L. Kane, Phys. Lett. 39B, 531 (1972); Nucl. Phys. B57, 157 (1973).
[8]G. A. Ringland, R. G. Roberts, D. P. Roy, and J. Tran Thanh Van, Nucl. Phys. B44, 395 (1972).
[9]S. Mandelstam, Nuovo Cimento 30, 1148 (1963).
[10]S.-P. Chia, Phys. Rev. D 5, 2316 (1972).
[11]S.-P. Chia, Phys. Rev. D 7, 1496 (1973).
[12]S.-P. Chia, ICTP, Trieste, Report No. IC/74/39 (unpublished).
[13]V. N. Gribov, Zh. Eksp. Teor. Fiz. 53, 654 (1967) [Sov. Phys.—JETP 26, 414 (1968)].
[14]L. M. Jones and P. V. Landshoff, Nucl. Phys. B94, 145 (1975).
[15]S.-P. Chia, ICTP, Trieste, Report No. IC/75/78 (unpublished).